Spring Chinook Status Assessment

McKenzie, Clackamas, and Sandy River Populations

A memorandum to

Fish Division
Oregon Department of Fish and Wildlife

Submitted

June 6, 2018
Matt Falcy, PhD
Fish Conservation Biologist
Oregon Department of Fish and Wildlife

Spring Chinook Status Assessment

McKenzie, Clackamas, and Sandy River Populations

This document describes the results and methods of population status assessments of spring Chinook in the McKenzie, Clackamas, and Sandy Rivers. Trend analyses, spawner-recruit analyses, and population viability analyses are described below. All data and computer code used to generate these results are available online: https://falcy.weebly.com/chinook-pva.html.

Contents

Primary Results

Table 1 presents results of a spawner trend analysis. Table 2 presents the median and standard deviation of recruits per spawner. Table 3 presents results of a PVA analysis. The remainder of this document describes how these results were obtained.

Table 1. *Spawner trends since 2002. Probabilities of decline in spawner abundance, point estimate of percent interannual change, and 95% highest probability density intervals around point estimates.*

	Population		
	McKenzie	Clackamas	Sandy
Probability of decline	0.998	0.34	0.02
Point Est of % annual change	-7.0	1.3	6.1
95% HPDI of % annual change	-11.1, -2.7	-5.2, 7.9	0.3, 11.9

Table 2. *Recruits per spawner since spawn-year 2002 under three different assumptions about the relative reproductive success (RRS) of hatchery-origin fish on the spawning grounds.*

	Population								
	McKenzie			Clackamas			Sandy		
	RRS=1	RRS=0.5	RRS=0	RRS=1	RRS=0.5	RRS=0	RRS=1	RRS=0.5	RRS=0
Median	0.51	0.65	0.89	0.94	0.97	1.01	0.81	1.04	1.36
SD	0.25	0.29	0.35	0.55	0.58	0.63	0.50	0.50	0.59

Table 3. *PVA results. Numerical entries are probabilities of quasi-extinction over a 100 year period. Scenarios include two different assumptions about the relative reproductive success (RRS) of hatchery-origin fish and two different statistical recruitment models. There is strong information-theoretic evidence that Model 2 is superior to Model 1. In the McKenzie, simulation scenarios included maximum observed California sea lion predation (CSL) and no California sea lion predation (CSL).*

	Population							
	McKenzie				Clackamas		Sandy	
	RRS=1		RRS=0.5		RRS=1	RRS=0.5	RRS=1	RRS=0.5
	Max CSL	No CSL	Max CSL	No CSL				
Model 1	0.35	0.23	0.28	0.22	0.007	0.006	0.010	0.004
Model 2	0.45	0.30	0.33	0.20	0.006	0.002	0.009	0.001

Overview

The purpose of this work is to assess the current population status of spring Chinook in the McKenzie, Clackamas, and Sandy River basins. The analyses are designed to facilitate comparisons among the populations on an "apples to apples" basis. Data prior to 2002 were not used because the proportion of hatchery-origin spawners in the McKenzie could not be reliably estimated, and the purpose of this work is to assess relatively contemporary conditions.

With a time series of spawner abundance, spawner age compositions, and mortality due to fishing and sea lions, it is possible to compute the adult recruits (progeny) associated with each year's spawner abundance. Density-dependence in these data was modeled with Ricker stock-recruitment functions. Two different Ricker models were used and information theoretic methods were used to determine the relative support in data for both models.

The Ricker models were fitted with Bayesian techniques in order to facilitate probabilistic interpretation of parameter estimates and their covariance. The estimated stock-recruitment relationship with parameter uncertainty and residual autocorrelation was combined with age composition and adult mortality data in order to project population dynamics through time in a population viability analysis (PVA). The PVA program takes 1000 random draws from the parameter posterior distribution of the stock recruitment model, and then replicates a 100-year time series 100 times. The total number of simulations where spawner abundance falls below a critical threshold across 4 consecutive year is divided by the total number of simulations (100,000). The result of this computation is the probability of quasi-extinction.

Scenarios in this assessment include different assumptions about the relative reproductive success (RRS, see inset) of hatchery fish, and effects of California sea lions (McKenzie population only).

Relative Reproductive Success

• • •

Assessments of population status are focused on natural-origin fish. The presence of hatchery origin fish on the spawning grounds makes it difficult to know how much production is attributable to natural-origin fish. The relative reproductive success (RRS) of hatchery fish on the spawning grounds is therefore an important parameter. As RRS goes down, more and more production must be coming from natural-origin fish.

Abundance Data

The abundance of natural and hatchery-origin spring Chinook in the in the Sandy and Clackamas rivers has been reported previously (ODFW 2017, Table 4). The McKenzie spring Chinook data were collated by the Willamette Salmonid Research, Monitoring, and Evaluation Program in ODFW. The abundance in the McKenzie River includes: (1) spawners above Leaburg Dam with a correction factor for fall back, (2) spawners below Leaburg Dam with a redd count expansion, and (3) spawners above and below Cougar Dam. Thus the entire McKenzie is treated as a single unit. For all populations, wild fish taken for broodstock are counted as recruits but not spawners.

Table 4. Basic abundance data used in this assessment. See also Figure 1.

	McKenzie		Clackamas		Sandy	
Year	Wild	Hatchery	Wild	Hatchery	Wild	Hatchery
2002	3361	1276	2140	948	919	201
2003	4178	1947	2633	730	871	125
2004	3982	1502	4051	1123	2416	88
2005	2135	832	1790	1092	1335	250
2006	2050	844	798	252	1070	114
2007	2562	1023	1175	480	1302	108
2008	1388	1044	1626	147	2722	2245
2009	1193	1347	754	64	856	965
2010	1265	2001	1251	90	1392	4686
2011	2511	1360	1588	178	1152	2287
2012	1769	1116	1729	101	2714	905
2013	1202	584	2133	101	1971	191
2014	1004	1049	915	69	1415	210
2015	1608	1268	2366	99	2728	219
2016	1716	1964	3376	104	3363	222
2017			3472	118		

Trend

Let the spawner abundance on year t, S_t, be a Poisson random variable:

$$p(S_t|\lambda) = \frac{\lambda^{N_t}e^{-\lambda}}{N_t!}.$$

Make the Poisson rate parameter, λ, a linear function of time on the log scale:

$$\lambda = e^{\alpha+\beta(t-\check{t})+\epsilon}.$$

The quantity $\check{t}$ is the midpoint of the time series, which simply centers the regressor to improve convergence. The quantity ϵ is zero-mean, normally distributed error:

$$p(\varepsilon|\sigma) = \frac{1}{\sqrt{2\pi\sigma^2}}e^{-\frac{\epsilon^2}{2\sigma^2}}.$$

Note that α and β play the roles of intercept and slope, respectively, in ordinary trend analysis. From here, we can define two additional quantities of interest. First, the predicted abundance is

$$\hat{S}_t = e^{\alpha+\beta(t-\check{t})+\frac{1}{2}\sigma^2}.$$

The term $\frac{1}{2}\sigma^2$ follows from probability theory used to translate the normal distribution across the log scale. The second quantity of interest is the geometric mean rate of interannual change (GMRIC). This is given on a percent scale by

$$GMRIC = 100\left(\left(\frac{S_{Tmax}}{S_{Tmin}}\right)^{\frac{1}{Tmax-Tmin}} - 1\right).$$

> ## Trend Analysis
>
> • • •
>
> A trend analysis simply uses time as a predictor of abundance. Extrapolating a trend forward through time tacitly assumes that conditions do not change. Here, observed trends are extrapolated into the future merely to illustrate recent observations. The extrapolations are not predictions about future abundance.

Box 1 provides the JAGS code used to fit the trend model described above. This model always has very nice convergence properties. A 95% highest probability density interval (HPDI) can be constructed from the posterior distribution of $\hat{S}_t$. Projecting the trend into the future is easily achieved by coding future observations of S_t as missing values (NA) and then making the Markov chain Monte Carlo simulation estimate them as parameters. Figure 1 gives the observed time series of spawner abundance and the 95% uncertainty envelope extrapolated into the future. Figure 2 presents the posterior distributions of GMRIC. Table 1 contains summary statistics of this trend analysis.

Box 1. JAGS code used to fit trend model

```
model{
for (t in 1:Nyears){
    log(lambda[t])<- alpha + beta*(t-fixedyear)+epsilon[t]
    N[t]~dpois(lambda[t])
    epsilon[t]~dnorm(0,tau_epsilon)
    fitted[t]<-exp(alpha+beta*(t-fixedyear)+0.5*sd_epsilon*sd_epsilon)
}
  ## Priors
  alpha~dnorm(0,1.0E-10)
  beta~dnorm(0,1.0E-6)
  #tau_epsilon~dgamma(0.001,0.001)#gamma used be be "uninformative" for tau
  tau_epsilon<-pow(sd_epsilon,-2) #tau=1/var
  sd_epsilon~dunif(0,6)#Gelman recommends uniform on SD

  ##Derived Params
  #sd_epsilon<-sqrt(1/tau_epsilon)
  B<-100*(pow(fitted[Nyears]/fitted[1],1/(Nyears-1))-1)
}
```
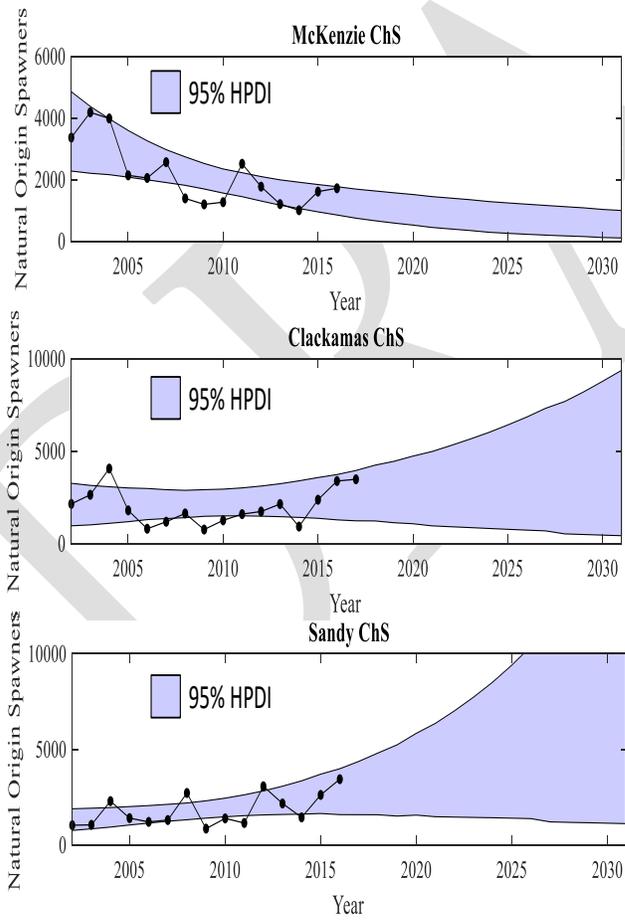

Figure 1. Trends through time in natural-origin spring Chinook spawners. Blue shaded area is a 95% highest probability density interval. See also Table 4.
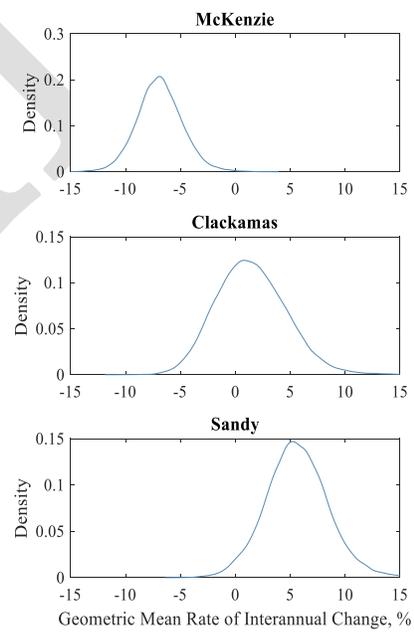

Figure 2. Posterior distributions of the annual rate of change in spawner abundance. The proportion of the area under each curve to the left of zero is the probability that the spawner abundance is declining during the period 2002-2016 (McKenzie and Sandy) or 2002-2017 (Clackamas). These probabilities are given in Table 1.

Mortality from Sea Lions- McKenzie

California sea lion predation on salmonids has been rigorously monitored by Wright et al. (2017) since 2014. Wright et al. (2017) note that the 2016 and 2017 estimates applied to just the "falls stratum" whereas monitoring in 2014 and 2015 included the fall and a "river stratum" just below the falls. Using information from years when both strata were monitored, it is possible to expand predation for 2016 and 2017 to include both strata. The resulting mortality of wild spring Chinook from 2014-2017 is: 496, 899, 1057, and 640. Dividing these mortality rates by spring Chinook abundances at the Willamette Falls counting window plus the estimates of mortality gives the "observed" mortality rates presented on the right-hand side of Figure 3.

Wright et al. (2014) note that predation losses of salmonids were generally a few hundred or less at the Falls from the late 1990s through 2003. Starting with 150 salmonid mortalities, I first expand for river stratum and then deflated the estimate by the mean proportion of all the salmonid mortality during 2014-2017 that are wild spring Chinook (15%). This yields the number of wild spring Chinook taken per year during this early period. This number is then expressed as the proportion of observed contemporary mortality rate. A linear assumption was used to connect
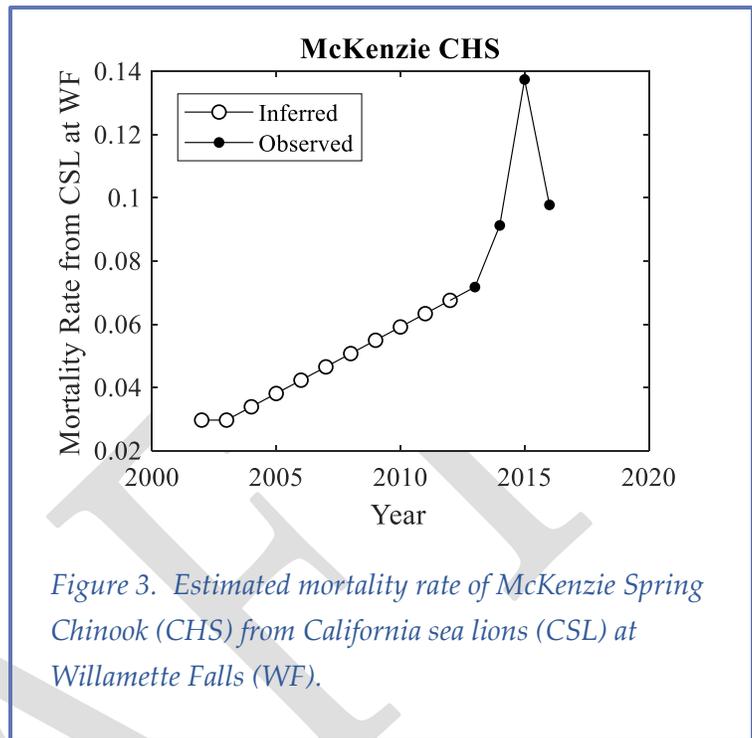

Figure 3. Estimated mortality rate of McKenzie Spring Chinook (CHS) from California sea lions (CSL) at Willamette Falls (WF).
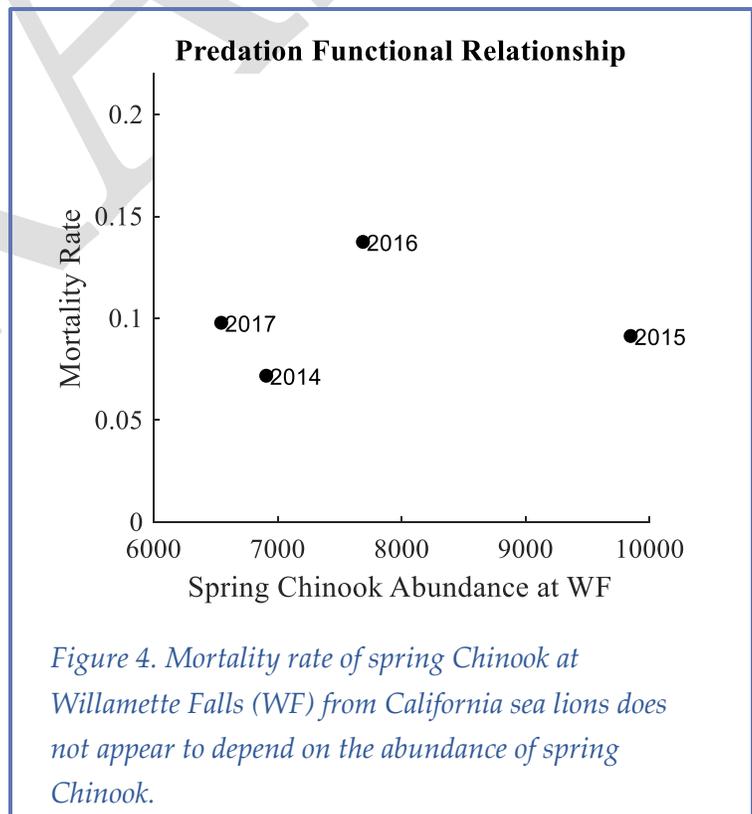

Figure 4. Mortality rate of spring Chinook at Willamette Falls (WF) from California sea lions does not appear to depend on the abundance of spring Chinook.

the early estimate of mortality rate to the to the 2014 estimate (left-hand side of Figure 3).

In the spawner-recruit analysis below, the mortality rate caused by sea lions on year t (denoted M_t below) is used to expand the recruits of McKenzie spring Chinook. The relationship between observed California sea lion predation rate on spring Chinook and the abundance of spring Chinook at Willamette Falls indicates a "Type I functional relationship" of predation (Figure 4). This relationship was used in the PVA for McKenzie spring Chinook.

Harvest

Freshwater harvest rates of wild spring Chinook in the Columbia and Willamette Rivers has been monitored since 2002 for compliance with the 2001 Fisheries Management and Evaluation Plan (ODFW 2017, Table 5). Incidental mortality on wild fish in the Sandy River was assumed to be 0.017 on all years. Total harvest rates for a population were computed as component products, reflecting the multiplicative survival process. For example, the freshwater harvest rate of McKenzie fish in 2017 is: 1- (1-0.014)*(1-0.001)*(1-0.024)*(1-0.001)*(1-0.002).

Table 5. Harvest rates used to compute recruits. From ODFW, 2017.

Year	Lower Columbia Commercial	Lower Columbia Recreational	Lower Willamette	Lower Clackamas	Upper Willamette	McKenzie
2002	0.024	0.011	0.03	0.049	0.003	0
2003	0.011	0.012	0.024	0.008	0.003	0.054
2004	0.042	0.01	0.027	0.003	0	0.019
2005	0.02	0.007	0.03	0.005	0.001	0.007
2006	0.08	0.008	0.043	0.003	0.001	0.014
2007	0.027	0.008	0.042	0.001	0.001	0.013
2008	0.005	0.002	0.048	0.002	0.001	0.001
2009	0.015	0.008	0.036	0.002	0.001	0.013
2010	0.06	0.018	0.069	0.002	0.002	0.01
2011	0.047	0.006	0.062	0.002	0.001	0.011
2012	0.025	0.01	0.045	0.003	0.002	0.013
2013	0.046	0.005	0.028	0.003	0.001	0.008
2014	0.03	0.009	0.039	0.001	0.001	0.005
2015	0.034	0.007	0.04	0.001	0.001	0.004
2016	0.016	0.003	0.022	0.001	0.001	0.005
2017	0.014	0.001	0.024	0.003	0.001	0.002

Ocean harvest was not incorporated into this analysis. This means that "recruits" are defined as the abundance of fish entering the Columbia River. Ocean fishing is therefore treated as an unknown stochastic process exactly like natural ocean mortality. The consequence of this assumption is that the mean and variance of ocean harvest rates since 2002 is perpetuated into the PVA.

Age Composition of Spawners

Age of spawning fish was determined through scale analysis. Age composition has been previously reported by ODFW (ODFW 2016, Table 6). The matrix of proportions of fish at age = 1,2,3, ..6, on given years (t) is denoted $A_{t,a}$ in the recruitment calculations below.

Table 6. *Age composition of spawners*

	McKenzie				Clackamas					Sandy			
Year	Age3	Age4	Age5	Age6	Age3	Age4	Age5	Age6	Age7	Age3	Age4	Age5	Age6
2002	0.01	0.69	0.30	0.00	0.00	0.59	0.39	0.02	0.00	0.00	0.46	0.51	0.03
2003	0.01	0.69	0.30	0.01	0.00	0.18	0.76	0.06	0.00	0.03	0.25	0.68	0.05
2004	0.01	0.54	0.45	0.00	0.00	0.45	0.53	0.02	0.00	0.00	0.74	0.25	0.00
2005	0.04	0.37	0.55	0.04	0.00	0.17	0.80	0.03	0.00	0.00	0.24	0.75	0.02
2006	0.00	0.68	0.30	0.02	0.00	0.49	0.47	0.04	0.01	0.01	0.41	0.57	0.01
2007	0.19	0.45	0.37	0.00	0.00	0.35	0.59	0.06	0.00	0.01	0.23	0.74	0.02
2008	0.24	0.64	0.11	0.00	0.01	0.35	0.61	0.03	0.00	0.00	0.43	0.55	0.02
2009	0.00	0.86	0.13	0.01	0.00	0.39	0.57	0.04	0.00	0.00	0.42	0.55	0.03
2010	0.14	0.57	0.29	0.00	0.01	0.32	0.63	0.04	0.00	0.05	0.43	0.51	0.00
2011	0.04	0.85	0.11	0.00	0.01	0.42	0.56	0.02	0.00	0.03	0.59	0.36	0.02
2012	0.06	0.52	0.40	0.02	0.01	0.34	0.60	0.05	0.00	0.00	0.55	0.43	0.02
2013	0.10	0.79	0.11	0.01	0.04	0.18	0.76	0.02	0.00	0.02	0.32	0.64	0.02
2014	0.11	0.62	0.26	0.01	0.09	0.59	0.30	0.01	0.00	0.03	0.51	0.46	0.01
2015	0.14	0.77	0.09	0.00	0.05	0.72	0.22	0.02	0.00	0.06	0.67	0.26	0.01
2016	0.15	0.61	0.25	0.00	0.03	0.57	0.40	0.00	0.00	0.07	0.66	0.27	0.00

Spawner-Recruit Analysis

The abundance of naturally produced ("wild") adult recruits associated with fish spawning on year *t* is

$$R_{S(t)} = \sum_{a=1}^{6} A_{t+a,a} \left(\frac{S_{t+a} * (1 - pHOS_{t+a})}{(1 - HR_{t+a}) * (1 - M_t)} \right).$$

From here it is possible to fit nonlinear models of the relationship between recruits and spawners. Errors in such models are customarily lognormal, reflecting the multiplicative survival processes that gives rise to uncertainty in the number of recruits. Summary statistics of recruits per spawner are given in Table 2.

Bayesian methods were adopted for recruitment modeling for two related reasons. First, Bayesian analysis uniquely yields probabilistic interpretation of parameters. Second, the Markov chain Monte Carlo (MCMC) methods used to fit Bayesian models allow parameter uncertainty to be easily folded into a PVA simulations. JAGS software was used to run the MCMC. JAGS called from MATLAB using matjags.m.

Ricker models were used to model spawner-recruit relationships (Table 7). Data from all three populations were combined into a "single" recruitment model. Two such models were constructed that make different assumptions about the error (Table 7). Model 1 assumes all parameters are unique to each population. Model 1 is equivalent to fitting a model to each population separately. Model 2 assumes there is a single error variance shared by all three populations, but each population has a unique productivity (α) and rate of compensatory density dependence (β). It is technically possible to construct a model that assumes that productivity is identical across populations. This may be prudent in many circumstances. However, this was not done here because there is an explicit focus on potential differences between populations and because there are significant geographical and hydrological differences between populations.

In both models, diffuse (noninformative) uniform priors were used for α (Unif(0.001,20)), β (Unif(0,0.1)), and the standard deviation ε (Unif(0,4)). Four MCMC chains per model were ran. The first 35,000 iterations were discarded as a "burn-in" period, and 10,000 samples per chain were retained after thinning 1:13 samples from the MCMC. Trace plots of the MCMC were visually inspected for signs of mixing and convergence. Extremely good estimates of the Gelman-Ruben diagnostic ($\hat{R} = 1 \mp 0.0001$) were obtained.

Watanabe-Akaike Information Criterion (WAIC) can be used to assess the relative out-of-sample predictive performance of Bayesian models

Table 7. Two Ricker recruitment models fitted to three populations of spring Chinook spawner-recruit data. The models make different assumptions about the number and structure of necessary parameters. Subscripts p and t denote population and time (year), respectively. WAIC measures relative out-of-sample predictive performance.

ID	Model	# Params	WAIC
1	$R_{t,p} = \alpha_p S_{t,p} e^{-\beta_p S_{t,p}} e^{\epsilon} , \epsilon \sim N\left(0, \sigma_p\right)$	9	466
2	$R_{t,p} = \alpha_p S_{t,p} e^{-\beta_p S_{t,p}} e^{\epsilon} , \epsilon \sim N\left(0, \sigma\right)$	6	481

(Gelman, Whang, and Vehtari, 2013). Each iteration of the MCMC yields a draw from the multidimensional posterior distribution. This parameter vector can be used to compute the probability density of each datum in the data set. This produces I-by-S matrix of densities, where I is the number of data points, and S is the arbitrary number of MCMC samples in the posterior. Armed with this matrix, the computed log pointwise predictive density is

$$lppd = \sum_{i=1}^{I} log\left(\frac{1}{S}\sum_{s=1}^{S} p(y_i|\theta^s)\right).$$

A correction for effective number of parameters to adjust for overfitting is obtained with

$$pwaic = \sum_{i=1}^{I} V_{s=1}^{S}(\log p(y_i|\theta^s)),$$

where V is the sample variance. Thus *pwaic* is just the posterior variance (across MCMC iterations) of the log predictive density for each data point, summed over all data points, and

$$WAIC = -2*(lppd\text{-}pwaic).$$

The units of WAIC can be interpreted like the more familiar AIC and DIC. Specifically, smaller values indicate better models. Model 2 is 15 units less than Model 1 (Table 7), indicating that it is a significantly superior model. The fit of Ricker Model 2 to the spawner-recruit data is given in Figure 5. Uncertainty in Ricker parameters gives rise to multiple potential recruitment functions. Random draws from the MCMC output ensures that parameter values and parameter covariance are obtained in proportion to the associated posterior probability densities.
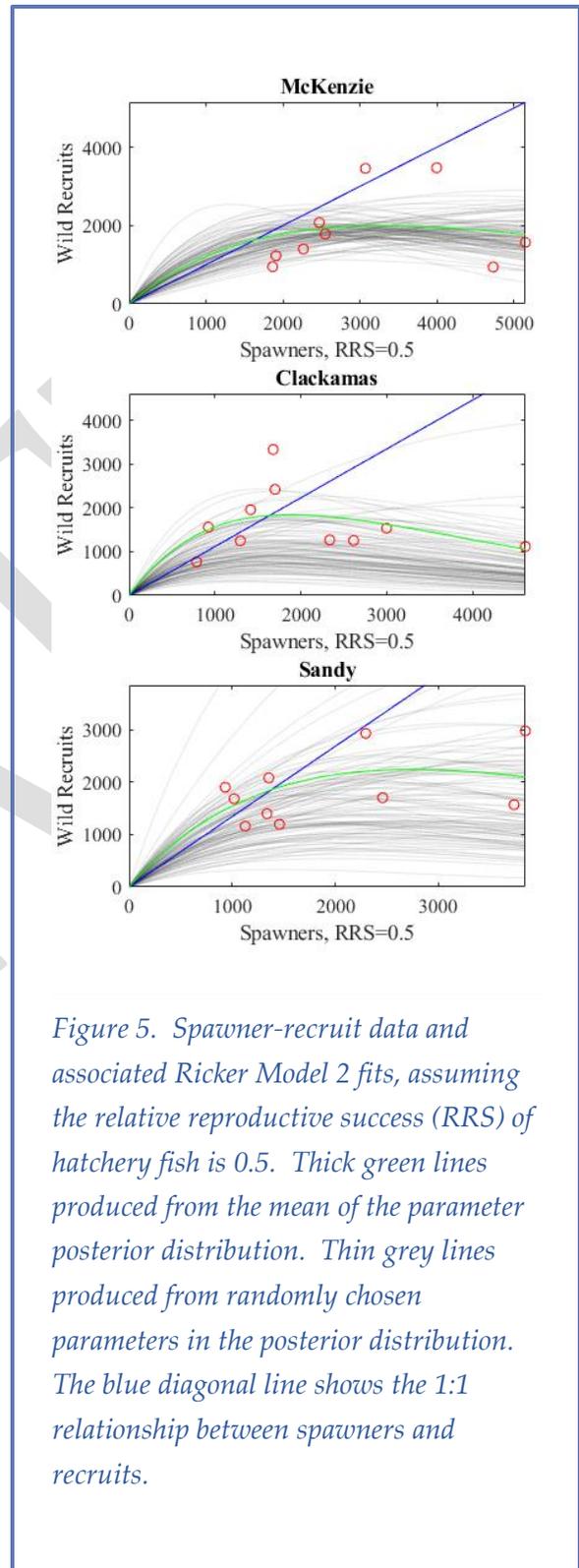

Figure 5. Spawner-recruit data and associated Ricker Model 2 fits, assuming the relative reproductive success (RRS) of hatchery fish is 0.5. Thick green lines produced from the mean of the parameter posterior distribution. Thin grey lines produced from randomly chosen parameters in the posterior distribution. The blue diagonal line shows the 1:1 relationship between spawners and recruits.

PVA

The population viability analysis (PVA) model use here was also used in a previous assessment of coastal fall Chinook (ODFW 2014) and Willamette winter steelhead (Falcy 2017). The PVA is a computer model that uses information from the spawner-recruit analysis (see previous section) to project/simulate population abundances into the future. 100,000 repetitions of the 100-year simulation are conducted, and the fraction of these that result in an extinction event yields the probability of extinction. It is important to note that the word "extinction" refers to a population (i.e. "local extinction", or "extirpation"), not a species.

The PVA was ran under different scenarios for each population. In the scenario called "No CSL" (Table 3) it is assumed that there is no additional mortality beyond the incidental angling mortality during the adult life stage. This assumption holds for all 100 years in the simulation. The scenario called "Max CSL" perpetuates the highest mortality rate observed since 2014 for all 100 years of the PVA simulation.

The Ricker recruitment function that is fitted to each population is the model of intergenerational population dynamics that is used within the PVA to simulate spawner abundances through time. However, in the spawner-recruit analysis, "recruits" are defined as pre-angling and pre-sea lion adults. The very same inland mortality estimates that are used to estimate adult recruits from spawner abundances are also used by the PVA to convert adult recruits back into spawners. Indeed, the analytical steps used to estimate recruits for the spawner-recruit analysis are reversed inside the PVA. The PVA

Population Viability Analysis

• • •

Population viability analysis (PVA) can be broadly defined as the use of quantitative methods to predict the future status of populations under defined conditions or scenarios. Here, a PVA is used to determine the probability of quasi-extinction over a 100 year period. The PVA scenarios explore different assumptions about RRS and the effects of sea lions at Willamette Falls (McKenzie only).

1. takes a given spawner abundance on year t,
2. uses the recruitment function to compute adult recruits,
3. recruits are apportioned across years according to random permutations of the age composition data,
4. recruits are summed across ages within a year and then deflated by harvest rate and sea lion mortality (if any).

A critically important aspect of all PVAs is the incorporation of stochasticty ("randomness"). Indeed, if stochasticity is neglected, then the steps outlined above would quickly result in static

population and extinction risk would be zero. Stochasticity enters the PVA in several ways. First, the spawner-recruit data are ambiguous with respect to the parameters of the recruitment function (Figure 5). Thus, uncertainty in the estimates of recruitment parameters α and β are simulated within the PVA by repeating simulations with 1000 different values of α and β. The 1000 different values of α and β are selected in proportion to the probabilities of different values and their covariance. This is accomplished by fitting the Ricker spawner-recruit model with MCMC methods in a Bayesian context. Samples of the MCMC are saved, and the PVA randomly selects parameter values out of this pool.

   The spawner-recruit data are not fully explained by the Ricker recruitment function, even though parameter uncertainty is acknowledged. In Figure 5, this can be seen as the vertical distances between spawner-recruit "points" and the line(s) representing the recruitment function(s). These "residual" deviations must also be simulated in the PVA. These residuals are lognormally distributed (note that the errors, ε, are exponentiated in the recruitment functions described above) and contain temporal autocorrelation. After the PVA receives a set of values for α and β, the variance of the errors is computed as well as the lag-1 autocorrelation of the errors. A 100-year time series of residual errors is then simulated using:

$$\varepsilon_t = \rho\varepsilon_{t-1} + \sqrt{\sigma^2}\sqrt{1-\rho^2}z_t \, ,$$

where ρ is the lag-1 autocorrelation of the errors, σ^2 is the variance of the errors, and z_t is a standard normal random deviate (Morris and Doak 2002, p. 139). These simulations are repeated 100 times for each of the 1000 random parameter draws. There are therefore 100*1000=100,000 repetitions of a 100-year time series.

   Extinction in the PVA model occurs when spawner abundance for four consecutive years falls below a "quasi-extinction threshold" (QET). A separate process called "reproductive failure threshold" (RFT) is used to zero-out recruitment at critically low spawner abundances. Both of these thresholds are implemented because processes like inbreeding depression, genetic drift, mate finding, and increased per-capita juvenile mortality will drive the population into extinction at critically low abundances. These negative density-dependent processes are very infrequently observed in nature, so they cannot be cannot be explicitly modeled. Collectively, both QET and RFT represent the boundary of an "extinction vortex" from which real populations are irrecoverable   (Gilpin and Soulé1984, Courchamp et al. 2008, Jamieson and Allendorf 2012). The specific values used here are RFT=QET=100. The PVA counts the fraction of the 100,000 simulations where adult abundance falls below QET across 4 consecutive years.

   The PVA model uses past abundances to infer extinction risk. Thus, the interpretation of the result is couched in the assumption that the conditions that were present when the data were collected will persist for 100 years. The model is not intended to capture effects of global warming, human

population growth, or other anticipated future change. Of course, the future will not be like the past. Future food webs are uncertain, as is the adaptive potential of these fish. The purpose of the PVA is not to forecast the future; rather, the PVA is useful for comparing the current status among populations and for comparing scenarios

The PVA needs to replicate observed patterns of variation in spawner abundance. A crude but effective method to determine if the PVA adequately captures observed population dynamics is to simply plot a randomly selected 100 year time series of simulated abundances and then superimpose the empirically observed/reconstructed abundances (Figure 6).   This visual test indicates that the PVA performs well. It simulates abundances that are greater and less than the empirical abundances, the
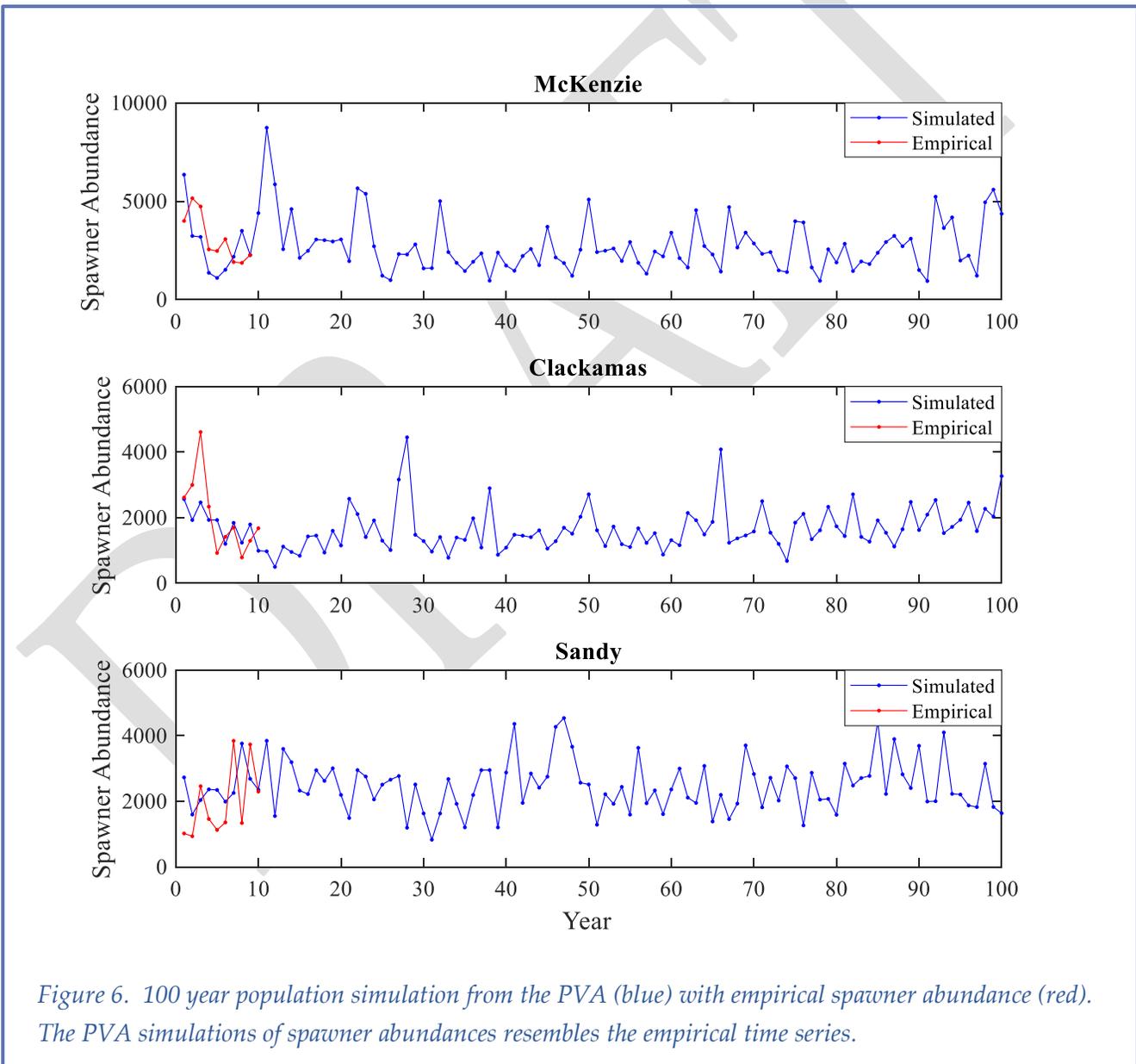

Figure 6. 100 year population simulation from the PVA (blue) with empirical spawner abundance (red). The PVA simulations of spawner abundances resembles the empirical time series.

volatility of these deviations seems to match the volatility of the empirical abundances, and the average simulated abundance approximates the average of the empirical abundances.

Uncertainty

The PVA produces a single number- the probability of quasi-extinction over 100 years. There are no confidence intervals. A confidence envelope could have been constructed if only the point estimate of the recruitment function had been used. However, in this Bayesian analysis, it is possible to describe parameter uncertainty probabilistically. Parameter uncertainty collapses into the final extinction probability by repeating PVA runs while sampling parameters from the posterior.

Simulations are repeated because there are stochastic processes that create alternative outcomes. This form of uncertainty can be made arbitrarily small simply by increasing the amount of simulation replication. Simulation uncertainty is on the order of the decimal degrees of rounding in Table 3.

Model uncertainty is addressed in Table 7 with WAIC. Table 3 presents the PVA results of Model 1 to demonstrate sensitivity to model choice. Information theoretic evidence indicates that Model 2 is much superior. Of course, there are other potential models of these data that others could elaborate if they are interested.

Discussion

It is noteworthy that there is only one year since 2002 when McKenzie spring Chinook recruitment exceeded replacement (Figure 5). There are no data points to support the model assumption that recruitment in the McKenzie exceeds replacement at low spawner abundances. Indeed, there is very little evidence for density dependence for these fish. If a density independent PVA had been used, then extinction would be guaranteed and average time to the extinction would be the metric output. The results presented here are conservative in the sense that survival of McKenzie spring Chinook are assumed to increase when spawner abundance is very low. If this is not the case, then extinction risk is actually much worse.

Acknowledgements

Luke Whitman provided critical insights into some of the data used here.

References

Courchamp, F., L. Berec, and J. Gascoigne. 2008. Allee effects in Ecology and Conservation. Oxford University Press, Oxford, UK.

Falcy, M.R. 2017. Population Viability of Willamette River Winter Steelhead: An assessment of the effects of sea lions at Willamette Falls.
https://falcy.weebly.com/uploads/1/1/4/9/114983925/willamettesthd.pdf

Gelman, A., J. Hwang, and A. Vehtari. 2014. Understanding predictive information criteria for Bayesian models. Statistics and computing 24: 997-1016.

Gilpin, M.E. and M.E. Soulé. 1984. Minimum viable populations: processes of species extinction. Pp 19-34 In Soulé, M.E. (Ed.). Conservation Biology: the science of scarcity and diversity. Sinauer, Sunderland, MA.

Jamieson, I.G. and F.W. Allendorf. 2012. How does the 50/500 rule apply to MVPs? Trends in Ecology and Evolution. 27:578-584.

Morris, W.F., and D.F. Doak. 2002. Quantitative Conservation Biology: Theory and practice of population viability analysis. Sinauer Associates.

ODFW 2014. Oregon Department of Fish and Wildlife. Coastal Multi-Species Conservation and Management Plan. Appendix II:
http://www.dfw.state.or.us/fish/CRP/docs/coastal_multispecies/CMP_main_final.pdf

ODFW 2016. Oregon Department of Fish and Wildlife. Progress Report: Spring Chinook Salmon in the Willamette and Sandy Basins.
https://odfw.forestry.oregonstate.edu/willamettesalmonidrme/sites/default/files/2016_sandy_basin_spring_chinook_spawning_survey.pdf

ODFW 2017. Oregon Department of Fish and Wildlife. Fisheries Management and Evaluation for 2017 Willamette River Spring Chinook.

Wright, B., T. Murtagh, and R. Brown. 2014. Willamette Falls Pinniped Monitoring Project.
http://www.dfw.state.or.us/fish/SeaLion/docs/Willamette%20Falls%202014%20sea%20lion%20report.pdf

Wright, B., T. Murtagh, R. Brown, and S. Riemer. 2017. Willamette Falls Pinniped Monitoring Project, 2017. https://www.dfw.state.or.us/fish/sealion/docs/Willamette_Falls_2017_sea_lion_report.pdf